

## Argenteanones C–E and Argenteanols B–E, Cytotoxic Cycloartanes from *Aglaia argentea*

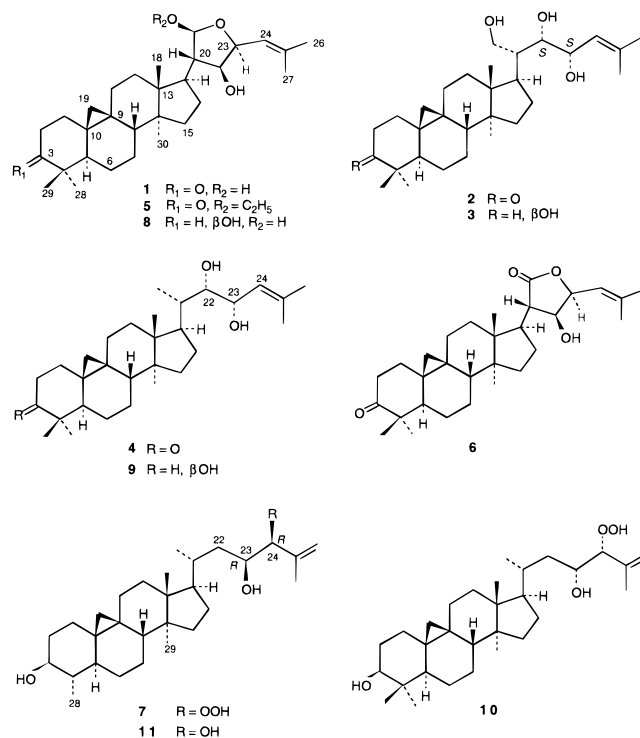
K. Mohamad,<sup>†</sup> M.-T. Martin,<sup>†</sup> E. Leroy,<sup>†</sup> C. Tempête,<sup>†</sup> T. Sévenet,<sup>†</sup> K. Awang,<sup>‡</sup> and M. Païs\*,<sup>†</sup>

*Institut de Chimie des Substances Naturelles, CNRS, 91198 Gif-sur-Yvette Cedex, France, and Department of Chemistry, University of Malaya, 59100 Kuala Lumpur, Malaysia*

Received August 26, 1996<sup>®</sup>

Seven new cycloartanes, argenteanones C–E (**4–6**) and argenteanols B–E (**7–10**), have been isolated from *Aglaia argentea* leaves. All of these compounds possess significant cytotoxic activity against KB cells (IC<sub>50</sub> values between 3.7 and 6.2  $\mu\text{g/mL}$ ). Structure elucidation was performed by 2D NMR spectroscopy, aided by molecular modeling in the case of the side chain of compound **7**.

A systematic biological screening of Malaysian plant extracts<sup>1</sup> using KB cells has led to the chemical study of the EtOH extract from the leaves of *Aglaia argentea* Bl. (Meliaceae). Three cycloartanes have been isolated, argenteanones A (**1**) and B (**2**) and argenteanol A (**3**), two of which, **1** and **2**, possess cytotoxic properties against KB cells.<sup>2,3</sup> Further examination of the EtOH extract resulted in isolation of seven new minor triterpenoids (**4–10**), belonging to the same cycloartane type, with all of these compounds also exhibiting cytotoxic properties. Structure elucidation was achieved using spectroscopic methods, essentially 2D NMR. In addition, molecular modeling was used to establish the conformation of the side chain of compound **4** and the stereochemistry of the side chain of compound **7**.



## Results and Discussion

The EtOH extract of *Aglaia argentea* leaves was fractionated on Si gel with mixtures of  $\text{CH}_2\text{Cl}_2$  and MeOH. The cytotoxic fractions obtained with  $\text{CH}_2\text{Cl}_2$ –MeOH 98:2 and 95:5 were repeatedly chromatographed on Si gel yielding the known argenteanones A (**1**) and B (**2**) and argenteanol A (**3**), together with the seven new cycloartanes **4–10**.

Argenteanone C (**4**),  $[\alpha]_D +11^\circ$ , exhibited a  $[\text{M} + \text{Na}]^+$  peak at  $m/z$  479.3481 ( $\Delta$  2.0 mmu) in the HRFABMS corresponding to a molecular formula of  $\text{C}_{30}\text{H}_{48}\text{O}_3$ . The IR spectrum showed an absorption of a carbonyl at  $1709\text{ cm}^{-1}$ . The  $^1\text{H}$ -NMR spectrum revealed a pair of doublets at  $\delta$  0.58 and  $\delta$  0.78 ( $J = 4\text{ Hz}$ ), respectively, typical of a C-9,C-10 cyclopropyl methylene group of a 3-oxo-cycloartane.<sup>4</sup> Comparison of the  $^1\text{H}$ - and  $^{13}\text{C}$ -NMR data with those of argenteanones A (**1**) and B (**2**)<sup>2</sup> confirmed the cycloartanone skeleton. In addition, the  $^1\text{H}$ -NMR spectrum exhibited the signal of a vinyl proton at  $\delta$  5.30 (br d,  $J = 9\text{ Hz}$ ), together with the resonances of two geminal vinyl methyls at  $\delta$  1.75 and ( $\delta_{\text{C}}$  25.5 and 18.0), thus indicating the presence of a terminal dimethylvinyl group in the side chain. Apart from the four methyl singlets of the cycloartanone-fused ring moiety (Table 1), a methyl-group doublet ( $\delta$  0.88,  $J = 6.5\text{ Hz}$ ) was observed and most probably located at C-21. Finally, two oxymethine signals appeared at  $\delta$  3.58 (d,  $J = 9.5\text{ Hz}$ ;  $\delta_{\text{C}}$  75.6) and  $\delta$  4.35 (dd,  $J = 9.5$  and  $7.5\text{ Hz}$ ;  $\delta_{\text{C}}$  68.0). Analysis of the COSY spectrum indicated that these two methines should be placed at C-22 and C-23, respectively, and confirmed the location of Me-21. The structure of the side chain was also supported by the HMBC spectrum (Table 1), which showed the correlations H-22/C-21,C-23,C-24, H-23/C-22,C-24,C-25, and Me-21/C-17,C-20,C-22.

The usual H-20 $\beta$  configuration of cycloartane derivatives was established for **4** by the NOESY correlations H-18/H-20 and H-12/H-21. For the side chain, the *S*-stereochemistry at C-22 and C-23 could be deduced from the NOESY spectrum (Table 1).<sup>5</sup> The conformation of the side chain was refined using a molecular modeling procedure (see Experimental Section), which takes into account coupling constants and distance restraints derived from the observed NOEs. From 50 refined models, 19 were selected on the basis of their best agreement with the experimental data, that is, no violation greater than 0.1 Å of the NOE distance

\* To whom correspondence should be addressed. Phone: 33 01 6982309. FAX: 33 01 69077247. E-mail: Mary.Pais@icsn.cnrs-gif.fr.

<sup>†</sup> Institut de Chimie des Substances Naturelles, CNRS, 91198 Gif-sur-Yvette Cedex, France.

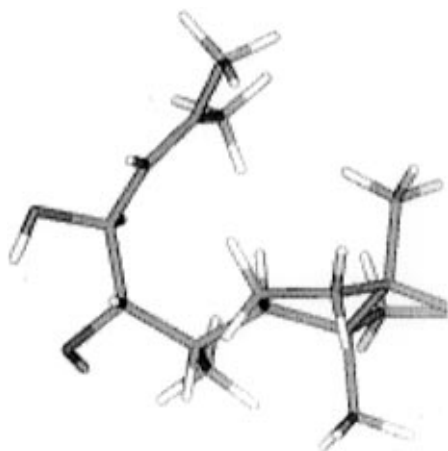
<sup>‡</sup> Department of Chemistry, University of Malaya, 59100 Kuala Lumpur, Malaysia.

<sup>®</sup> Abstract published in *Advance ACS Abstracts*, January 15, 1997.

**Table 1.**  $^{13}\text{C}$ - (62.5 MHz) and  $^1\text{H}$ -NMR (400 MHz) Data<sup>a</sup> for Argenteanone C (**4**) and Argenteanol B (**7**)

position	$\delta\text{C}^c$	$\delta\text{H}$ (J Hz) <sup>c</sup>	HMBC <sup>c</sup>	NOESY <sup>d</sup>	$\delta\text{C}$	$\delta\text{H}$ (J Hz)	HMBC	NOESY
1	32.9	$\alpha$ 1.85 m $\beta$ 1.55 m	10, 19 3, 5, 10	$1\beta$ , $2\alpha$ , $2\beta$ $2\alpha$ , $11\beta$ , $19\alpha$	31.8	$\alpha$ 1.48 m $\beta$ 1.23 m	10	$1\beta$ , $2\beta$ , 3
2	36.9	$\alpha$ 2.30 m $\beta$ 2.70 ddd (14,7,7)	3, 10 1, 3, 10	$2\beta$ 29	35.4	$\alpha$ 1.88 m $\beta$ 1.38 m	10 3	$2\beta$ , 3
3	216.8				77.0	3.12 ddd (10)		5, 28
4	49.7				44.7	1.08 m		28
5	47.8	1.70 m	1, 4, 9, 10, 19	28	45.3	1.13 m		$7\alpha$
6	20.9	$\alpha$ 1.55 m $\beta$ 0.90 m		$6\beta$ , 28 $7\beta$ , 8, $19\beta$	25.7	$\alpha$ 1.64 m $\beta$ 0.52 m		$6\beta$ , $7\alpha$ , 28 8, $19\beta$
7	25.3	$\alpha$ 1.10 m $\beta$ 1.35 m		$7\beta$	26.2	$\alpha$ 0.98 m $\beta$ 1.24 m		$7\beta$ , 30
8	47.1	1.60 m	9, 13, 14, 15, 19, 30	15, 18, $19\beta$	48.3	1.53 m	9, 10, 14, 15	18, $19\beta$
9	20.5				24.5			
10	25.4			30.6				
11	26.1	$\alpha$ 2.05 m $\beta$ 1.15 m	9, 10, 12, 19	$11\beta$ , 12, 30 12, $19\alpha$	27.9	$\alpha$ 1.90 m $\beta$ 1.14 m	9, 10, 12, 19 8, 12, 13	$11\beta$ , 12, 30 12
12	32.3	1.50 m		21	34.0	1.58 m	9, 11, 13, 18	21
13	45.1				46.5			
14	47.8			50.0				
15	35.2	1.30 m	16, 30	18, 30	36.3	1.23 m	30	
16	27.2	$\alpha$ 1.70 m $\beta$ 1.35 m		$16\beta$ , 22 22	28.9	$\alpha$ 1.84 m $\beta$ 1.25 m	15	$16\beta$ , 17 20
17	40.4	1.85 m	21	22, 24, 30	54.1	1.47 m		
18	17.0	0.95 s	12, 13, 14	20	18.4	0.95 s	12, 13, 14, 17	20
19	28.8	$\alpha$ 0.58 d (4) $\beta$ 0.78 d (4)	1, 5, 8, 9, 10, 11 1, 5, 8, 9, 10, 11	$19\beta$ 29	28.0	$\alpha$ 0.09d (3.8) $\beta$ 0.33d (3.8)	1, 5, 8, 9, 10, 11 1, 5, 8, 9, 10, 11	$19\beta$
20	47.8	1.80 m		21, 22	33.0	1.66 m		21
21	12.8	0.88 d (6.5)	17, 20, 22	23	18.3	0.82 d (7)	17, 20, 22	23, 26a
22	75.6	3.58 d (9.5)	21, 23, 24	24	40.6	$\alpha$ 1.44 m $\beta$ 0.85 m	21, 23	22b 24
23	68.0	4.35 dd (9.5, 7.5)	22, 24, 25	26, 27	68.5	3.68 dd (8.4, 10)		27
24	124.3	5.30 br d	26, 27	26, 27	95.4	4.00 d (8.4)	22, 23, 26, 27	26a
25	135.9				143.7			
26	25.5	1.75 s	24, 25, 27		116.3	a 4.96 br s b 4.99 br s	24, 25, 27 24, 27	26b 27
27	18.0	1.75 s	24, 25, 26		18.0	1.66 s	24, 25, 26	
28	21.6	0.98 s	3, 4, 5, 29		14.8	0.91 d (6)	3, 5	
29	20.0	1.05 s	3, 4, 5, 28		19.6	0.83 s	8, 13, 14, 15	
30	18.5	0.78 s	8, 13, 14, 15					

<sup>a</sup> Assignments are based on 2D experiments. <sup>b</sup> In  $\text{CDCl}_3$  +  $\text{CD}_3\text{OD}$ . <sup>c</sup> In  $\text{CDCl}_3$ . <sup>d</sup> In pyridine- $d_5$ .

**Figure 1.** Most-favored conformer of the side chain of argenteanone C (**4**) derived by molecular modeling.

restraints, no violation greater than  $10^\circ$  of the  $^3J$ -derived angle restraints, and lowest total energy. They all belong to a convergent family, and one of these models is shown in Figure 1.

Argenteanone D (**5**),  $[\alpha]_D +15^\circ$ , exhibited a  $[\text{M} + \text{Na}]^+$  ion at  $m/z$  521.3464 in the HRFABMS ( $\Delta -3.9$  mmu) in accordance with the elemental formula  $\text{C}_{32}\text{H}_{50}\text{O}_4$ . The IR spectrum showed a carbonyl absorption at  $1709\text{ cm}^{-1}$ , and the NMR spectral data were consistent with a cycloartan-3-one skeleton. The side chain was similar to the one previously found in argenteanone A (**1**),

showing the characteristic NMR signals (Table 2 and Experimental Section) of the hemiacetal ring and the terminal dimethylvinyl group. However, the hemiacetal carbon was shifted upfield ( $\delta$  105.6), and additional signals of an ethoxy group (Table 1) suggested that this group was attached to C-21. The HMBC correlations observed from one proton of the  $\text{CH}_2\text{O}$  group to C-21 confirmed this assignment. Finally, the NOESY cross peaks  $\text{CH}_3$ -18/H-20, H-16/H-22, H-17/H-23, and H-22/H-23 indicated that C-22 and C-23 both have the same *S*-configuration as the previous compound **1**.

Argenteanone E (**6**),  $[\alpha]_D -10^\circ$ , showed a  $[\text{M} + \text{Na}]^+$  peak at  $m/z$  491.3147 in the HRFABMS ( $\Delta -1.0$  mmu) that matched a molecular formula of  $\text{C}_{30}\text{H}_{44}\text{O}_4$ . The IR spectrum exhibited two carbonyl bands at 1702 and  $1775\text{ cm}^{-1}$ . The NMR spectra indicated a cycloartan-3-one skeleton (Table 2 and Experimental Section) and proved further the existence of a terminal *gem*-dimethylvinyl group similar to those of compounds **1**–**5**. The other signals were two oxymethines resonating at  $\delta_C$  74.9 and  $\delta_C$  79.0 and a carbonyl at  $\delta_C$  177.4. These data, together with the IR band at  $1775\text{ cm}^{-1}$  and the lack of the C-21 hemiacetal signal near  $\delta_C$  100, suggested that the hemiacetal ring of **1** was replaced by a lactone. This was confirmed by the COSY spectrum and the correlations H-20/C-21 and H-22/C-21 observed in the HMBC experiment. The *S*-stereochemistry at C-22 and C-23, which is similar to those of argenteanone A (**1**), was

**Table 2.**  $^{13}\text{C}$  NMR (62.5 MHz) Data for Compounds **5**, **6**, and **8–10** ( $\text{CDCl}_3$ )

carbon	<b>5</b> <sup>a</sup>	<b>6</b> <sup>a</sup>	<b>8</b> <sup>a</sup>	<b>9</b>	<b>10</b>
1	33.5	33.4	32.1	32.3	32.0
2	37.5	37.5	30.4	30.4	30.0
3	216.4	216.9	77.6	79.1	78.6
4	50.3	50.3	40.6	40.8	40.4
5	48.5	48.4	47.2	47.4	47.1
6	21.0	21.2	21.1	21.4	21.1
7	26.0	25.9	26.1	26.3	25.9
8	48.0	47.8	48.0	48.1	47.9
9	20.9	21.0	19.9	20.2	19.9
10	26.2	26.1	29.8	26.3	27.4
11	27.5	26.4	26.4	26.7	26.4
12	32.6	30.2	32.6	33.2	32.9
13	45.9	45.7	45.9	45.9	45.4
14	48.8	48.8	50.0	48.8	48.7
15	35.6	35.1	35.6	36.0	35.5
16	27.5	28.4	27.7	28.1	28.1
17	45.0	45.5	44.6	41.3	52.9
18	19.4	18.4	19.3	17.8	18.0
19	29.7	29.6	30.1	30.1	29.8
20	57.8	52.1	58.3	48.7	32.4
21	105.6	177.4	101.0	13.6	17.6
22	77.4	74.9	78.9	76.5	39.2
23	79.5	79.0	79.9	68.8	67.7
24	121.3	117.1	121.1	125.2	94.5
25	137.5	141.5	138.4	136.3	144.2
26	26.3	26.1	26.1	25.2	116.2
27	18.6	19.1	19.3	18.8	17.6
28	22.3	22.3	25.5	25.7	25.3
29	20.9	20.8	13.2	14.3	13.9
30	19.4	19.4	19.4	19.4	19.2
$\text{OCH}_2\text{CH}_3$	63.0				
$\text{OCH}_2\text{CH}_3$	15.4				

<sup>a</sup> Assignments are based on 2D experiments (COSY, HMQC, HMBC, NOESY).

deduced from the NOESY correlations H-16/H-22, H-17/H-23, and H-22/H-23.

Argenteanol B (**7**),  $[\alpha]_D^{+23}$ , showed a  $[\text{M} + \text{Li}]^+$  peak in the HRFABMS at  $m/z$  467.3753 ( $\Delta -4.0$  mmu) corresponding to a molecular formula of  $\text{C}_{29}\text{H}_{48}\text{O}_4$ . The carbonyl absorption in the IR spectrum was absent, and the two doublets of the cyclopropyl methylene group were shifted far upfield to values of  $\delta$  0.09 and 0.33 ( $J = 4$  Hz), respectively, characteristic of a  $4\beta$ -demethylcycloartan- $3\beta$ -ol.<sup>4</sup> The structure of the fused ring moiety was confirmed by the  $^{13}\text{C}$ - $^{6,7}$  and 2D NMR data (Table 1). Furthermore, the H- $3\alpha$  configuration was supported by the diaxial coupling constant between H-3 and H- $2\beta$  ( $J = 10$  Hz). For the side chain, the 1D NMR data together with the COSY and HMQC data (Table 1) were consistent with the presence of a terminal isopropenyl group, two oxymethines at position C-23 ( $\delta_{\text{H}}$  3.68, dd;  $\delta_{\text{C}}$  68.5) and C-24 ( $\delta_{\text{H}}$  4.00, d;  $\delta_{\text{C}}$  95.4), a methylene at C-22 and a Me-21 group. The HMBC cross peaks H-21/C-22 and H-22/C-24 confirmed these assignments. The downfield shift of C-24 suggested that a hydroperoxyl group was attached to this carbon.<sup>8</sup> The  $-\text{OOH}$  group was also proved by the presence of a broad singlet at  $\delta$  14.06 in the  $^1\text{H}$ -NMR spectrum (pyridine- $d_5$ ).<sup>8</sup> Reduction of compound **7** using triphenylphosphine yielded the corresponding hydroxy compound **11** ( $\delta_{\text{H-23}}$  3.69, ddd;  $\delta_{\text{H-24}}$  3.78, d).

The stereochemistry at C-23 and C-24 of **7** could not be established directly by the NOESY experiment. Therefore, molecular modeling calculations were used. Four models—*RR*, *RS*, *SR*, and *SS*—were built and refined as described in the Experimental Section. They led to four sets of refined models that were analyzed in

**Figure 2.** Most-favored conformer of the side chain of argenteanol B (**7**) derived by molecular modeling.

terms of their best agreement with the experimental data. The *23-R* and *24-R* models were selected with only one violation per model greater than 0.1 Å of the NOE distance restraints<sup>9</sup> and no violation greater than  $10^\circ$  of the  $^3J$  derived angle restraints. They represent a convergent energetical family of 50 models ( $214 \pm 1.5$  kcal/mol). The 14 lowest energy models were selected ( $213 \pm 1.5$  kcal/mol). One of them is presented in Figure 2. The *23-R* and *24-R* stereochemistry has been determined previously using other methods for alisol G,<sup>10,11</sup> a triterpenoid that possesses a side chain similar to that of compound **11**. Both triterpenes exhibit a closely related splitting pattern for H-23 (ddd,  $J = 6.5, 10.7, 1.7$  Hz for **11**) and H-24 (d,  $J = 6.5$  Hz for **11**). The NOESY spectrum of compound **11** showed, as was the case for compound **7**, the correlations H-21/H-23, H-24/H-26, and H-23/H-27, which are consistent with *R* stereochemistry for both H-23 and H-24.

The  $^1\text{H}$ -NMR spectra of argenteanols C–E (**8–10**) all displayed the typical highfield doublets of a cycloartan- $3\alpha$ -ol.<sup>2,4</sup> The  $^{13}\text{C}$ -NMR spectra (Table 2) of the fused-ring moiety were similar in each case to those of known cycloartan- $3\beta$ -ols, and the splitting pattern of H-3 confirmed the H- $3\alpha$  stereochemistry. The structures of the various side chains of compounds **8–10** were deduced from the HRFABMS (see Experimental Section) and from the  $^1\text{H}$ - and  $^{13}\text{C}$ -NMR data, which were similar to those of argenteanone A (**1**), argenteanone C (**3**), and argenteanol B (**7**), respectively.

Compounds **4–10** exhibited cytotoxicity in moderate potency against KB cells ( $\text{IC}_{50}$  values 4.1, 4.2, 3.7, 3.7, 6.2, 4.0, and 5.9  $\mu\text{g/mL}$ , respectively). Allylic hydroperoxyl cycloartanes have been recently isolated from *Tillandsia recurvata*<sup>12</sup> and *Tillandsia usneoides*.<sup>13</sup> These compounds and other naturally occurring hydroperoxides originate most probably from a natural oxygenation process.<sup>12,13</sup> The ethoxy compound argenteanone D (**4**) could be an artifact because EtOH was used to extract the plant material, although a natural origin cannot be ruled out.

## Experimental Section

**General Experimental Procedures.** Optical rotations at  $20^\circ\text{C}$  were obtained on a Perkin-Elmer 241 polarimeter. The various spectra were recorded on the following instruments: UV, Shimadzu UV-161 UV-vis spectrophotometer; IR ( $\text{CHCl}_3$ ), Nicolet 205 FT-IR spectrometer; FABMS, Kratos MS 80; HRFABMS, VG-Zab-Seq spectrometer; NMR, Bruker AC 250 ( $^1\text{H}$ - and  $^{13}\text{C}$ -NMR spectra) and AM 400 (2D NMR spectra). UV

spectra were recorded in MeOH. Column chromatography was performed using Si gel Merck H60.

**Plant Material.** Bark material of *Aglaia argentea* Bl. was collected in Dungun, Terengganu, Malaysia, in March 22, 1993. The identification was made by G. Perromat, Institut de Chimie des Substances Naturelles, CNRS, Gif-sur-Yvette. Voucher specimens (KL 4347) are deposited at the Laboratoire de Phanérogamie, Muséum National d'Histoire Naturelle in Paris; at the Herbarium of Department of Chemistry, University of Malaya, Kuala Lumpur, Malaysia; and at the Herbarium of the Forest Research Institute, Kepong, Malaysia.

**Extraction and Isolation.** The dried ground leaves of *A. argentea* (200 g) were extracted exhaustively with EtOH at room temperature. The extract (19.6 g) was chromatographed on Si gel (70–200 mesh) with mixtures of  $\text{CH}_2\text{Cl}_2$ –MeOH as eluents. Four successive fractions were eluted using  $\text{CH}_2\text{Cl}_2$ –MeOH (98:2) with fractions II–IV showing significant cytotoxicity against KB cells (70% inhibition at 10  $\mu\text{g/mL}$ ). Accordingly, these fractions were subjected to further Si gel (Merck H 60) chromatography with mixtures of heptane–EtOAc or heptane– $\text{Me}_2\text{CO}$ . Fraction II yielded **5** (40 mg) (heptane–EtOAc 9:1) and **6** (10 mg) (heptane–EtOAc 8:2). Fraction III yielded **4** (10 mg) (heptane–EtOAc 7:3) and **8** (12 mg) (heptane–EtOAc 6:4). Fraction IV yielded **9** (11 mg) (heptane–EtOAc 8:2 followed by heptane–EtOAc 8:2), **7** (10 mg) (heptane–EtOAc 8:2 followed by heptane–EtOAc 8:2), and **1** (325 mg) (heptane–EtOAc 6:4). The fraction eluted with  $\text{CH}_2\text{Cl}_2$ –MeOH (95:5), which also showed activity against KB cells, was further fractionated, yielding **9** (21 mg) (heptane– $\text{Me}_2\text{CO}$  85:15), **2** (36 mg) (heptane– $\text{Me}_2\text{CO}$  8:2 followed by heptane–EtOAc 8:2), and **3** (21 mg) (heptane– $\text{Me}_2\text{CO}$  1:1 followed by  $\text{CH}_2\text{Cl}_2$ –MeOH 95:5).

**Argenteanone C (4):** amorphous solid;  $[\alpha]_{\text{D}} +11^\circ$  (*c* 1,  $\text{CHCl}_3$ ); IR  $\nu_{\text{max}}$  3410, 1709  $\text{cm}^{-1}$ ;  $^1\text{H}$ - and  $^{13}\text{C}$ -NMR data in  $\text{CDCl}_3$ , see Table 1;  $^1\text{H}$ -NMR (pyridine-*d*<sub>5</sub>)  $\delta$  0.50 (1H, d,  $J = 4$  Hz, H-19 $\alpha$ ), 0.66 (1H, d,  $J = 4$  Hz, H-19 $\beta$ ), 2.02 (1H, m, H-16 $\alpha$ ), 1.48 (1H, m, H-16 $\beta$ ), 2.02 (1H, m, H-17), 2.18 (1H, m, H-20), 1.29 (3H, d,  $J = 6.8$ , H-21), 3.98 (1H, dd,  $J = 7.5$ , 2.5 Hz, H-22), 4.73 (1H, dd,  $J = 7.5$ , 9.5 Hz, H-23), 5.70 (1H, br d,  $J = 9.5$ , H-24); all assignments in pyridine-*d*<sub>5</sub> were based on COSY, HMQC, and HMBC correlations; FABMS  $m/z$  479  $[\text{M} + \text{Na}]^+$ ; HRFABMS  $m/z$  479.3481 ( $\text{C}_{30}\text{H}_{48}\text{NaO}_3$ ,  $\Delta$  2.0 mmu).

**Argenteanone D (5):** amorphous powder;  $[\alpha]_{\text{D}} +12.6^\circ$  (*c* 1,  $\text{CHCl}_3$ ). IR  $\nu_{\text{max}}$  3400, 1709  $\text{cm}^{-1}$ ;  $^1\text{H}$  NMR ( $\text{CDCl}_3$ )  $\delta$  2.28 (1H, m, H-2 $\alpha$ ), 2.70 (1H, ddd,  $J = 14$ , 14, 6.5 Hz, H-2 $\beta$ ), 1.95 (1H, m, H-16 $\alpha$ ), 1.55 (1H, m, H-16 $\beta$ ), 1.80 (1H, m, H-17), 1.08 (3H, s, H-18), 0.57 (1H, d,  $J = 4.4$  Hz, H-19 $\alpha$ ), 0.78 (1H, d,  $J = 4.4$ , H-19 $\beta$ ), 4.97 (1H, s, H-21), 3.87 (1H, dd,  $J = 11$ , 4.5 Hz, H-22), 4.75 (1H, dd,  $J = 9$ , 4.5 Hz, H-23), 5.40 (1H, dt,  $J = 9$ , 1, H-24), 1.70 (3H, d,  $J = 1$  Hz, H-26), 1.78 (3H, d,  $J = 1$  Hz, H-27), 1.02 (3H, s, H-28), 1.05 (3H, s, H-29), 0.90 (3H, s, H-30), 3.40 (1H, dq,  $J = 16$ , 8,  $\text{CH}_2\text{Oa}$ ), 3.78 (1H, dq,  $J = 16$ , 8,  $\text{CH}_2\text{Ob}$ ), 15.4 (3H, t,  $J = 7$ ,  $\text{CH}_3\text{CH}_2\text{O}$ );  $^{13}\text{C}$ -NMR data, see Table 2; HMBC correlations: H-21/C-17, C-20, C-22, C-23,  $\text{CH}_2\text{O}$ ; H-22/C17, C-21, C-23; H-23/C-21, C-24, C-25; H-24/C-26, C-27;  $\text{CH}_2\text{Ob}$ /C-21; FABMS  $m/z$  521  $[\text{M} + \text{Na}]^+$ ; HRFABMS  $m/z$  521.3464 ( $\text{C}_{30}\text{H}_{50}\text{NaO}_4$ ,  $\Delta$  -3.9 mmu).

**Argenteanone E (6):** amorphous powder,  $[\alpha]_{\text{D}} -10^\circ$  (*c* 1,  $\text{CHCl}_3$ ); IR  $\nu_{\text{max}}$  3410, 1775, 1702  $\text{cm}^{-1}$ ;  $^1\text{H}$  NMR ( $\text{CDCl}_3$ )  $\delta$  2.30 (1H, m, H-2 $\alpha$ ), 2.70 (1H, m, H-2 $\beta$ ), 1.22 (3H, s, H-18), 0.55 (1H, d,  $J = 4$  Hz, H-19 $\alpha$ ), 0.78 (1H, d,  $J = 4$ , H-19 $\beta$ ), 2.65 (1H, m, H-20), 4.20 (1H, d,  $J = 3.6$  Hz, H-22), 5.20 (1H, dd,  $J = 8$ , 3.6 Hz, H-23), 5.35 (1H, dt,  $J = 8$ , 1 Hz, H-24), 1.82 (3H, s, H-26), 1.75 (3H, s, H-27), 1.02 (3H, s, H-28), 1.08 (3H, s, H-29), 0.90 (3H, s, H-30);  $^{13}\text{C}$ -NMR data, see Table 2; HMBC correlations H-20/C-16, C-17, C-22, C-23; H-22/C17, C-21, C-23; H-23/C-24; H-24/C-26, C-27; FABMS  $m/z$  491  $[\text{M} + \text{Na}]^+$ ; HRFABMS  $m/z$  491.3147 ( $\text{C}_{30}\text{H}_{44}\text{NaO}_4$ ,  $\Delta$  -1.0 mmu).

**Argenteanol B (7):** amorphous powder,  $[\alpha]_{\text{D}} +23^\circ$  (*c* 1,  $\text{CHCl}_3$ );  $^1\text{H}$ - and  $^{13}\text{C}$ -NMR data, see Table 1; FABMS  $m/z$  467  $[\text{M} + \text{Li}]^+$ ; HRFABMS  $m/z$  467.3753 ( $\text{C}_{29}\text{H}_{48}\text{LiO}_4$ ,  $\Delta$  -4.0 mmu).

**Argenteanol C (8):** amorphous powder,  $[\alpha]_{\text{D}} +16^\circ$  (*c* 0.2,  $\text{CHCl}_3$ );  $^1\text{H}$ -NMR ( $\text{CDCl}_3$ )  $\delta$  3.30 (1H, m,  $W_{1/2} = 10$  Hz, H-3), 1.12 (3H, s, H-18), 0.38 (1H, d,  $J = 4$  Hz, H-19 $\alpha$ ), 0.60 (1H, d,  $J = 4$ , H-19 $\beta$ ), 2.42 (1H, d,  $J = 12$ , H-20), 5.35 (1H, d,  $J = 7$  Hz, H-21), 4.20 (1H, dd,  $J = 4$ , 4, H-22), 4.80 (1H, dd,  $J = 8$ , 4 Hz, H-23), 5.45 (1H, br d,  $J = 8$ , H-24), 1.82 (3H, s, H-26), 1.75 (3H, s, H-27), 0.82 (3H, s, H-28), 0.98 (3H, s, H-29), 0.92 (3H, s, H-30);  $^{13}\text{C}$ -NMR data, see Table 2; FABMS  $m/z$  495  $[\text{M} + \text{Na}]^+$ ; HRFABMS 495 3487 ( $\text{C}_{30}\text{H}_{48}\text{NaO}_4$ ,  $\Delta$  -3.7 mmu).

**Argenteanol D (9):** amorphous powder,  $[\alpha]_{\text{D}} +24^\circ$  (*c* 1,  $\text{CHCl}_3$ );  $^1\text{H}$  NMR ( $\text{CDCl}_3$ )  $\delta$  3.30 (1H, dd,  $J = 10$ , 4, H-3), 0.98 (3H, s, H-18), 0.32 (1H, d,  $J = 4$  Hz, H-19 $\alpha$ ), 0.55 (1H, d,  $J = 4$ , H-19 $\beta$ ), 0.82 (3H, d,  $J = 7$  Hz, H-21), 3.55 (1H, d,  $J = 9$ , H-22), 4.30 (1H, dd,  $J = 8$ , 8 Hz, H-23), 5.25 (1H, br d,  $J = 10$ , H-24), 1.78 (3H, s, H-26), 1.78 (3H, s, H-27), 0.82 (3H, s, H-28), 0.98 (3H, s, H-29), 0.98 (3H, s, H-30);  $^{13}\text{C}$ -NMR data, see Table 2; FABMS  $m/z$  481  $[\text{M} + \text{Na}]^+$ ; HRFABMS  $m/z$  481.3671, ( $\text{C}_{30}\text{H}_{50}\text{NaO}_3$ ,  $\Delta$  -3.3 mmu).

**Argenteanol E (10):** amorphous powder,  $[\alpha]_{\text{D}} +29^\circ$  (*c* 1,  $\text{CHCl}_3$ );  $^1\text{H}$  NMR ( $\text{CDCl}_3$ )  $\delta$  3.26 (1H, dd,  $J = 10$ , 4 Hz, H-3), 0.97 (3H, s, H-18), 0.31 (1H, d,  $J = 4$  Hz, H-19 $\alpha$ ), 0.54 (1H, d,  $J = 4$ , H-19 $\beta$ ), 0.82 (3H, d,  $J = 7$  Hz, H-21), 3.77 (1H, ddd,  $J = 11$ , 8.2, 1.5 Hz, H-23), 4.14 (1H, d,  $J = 8.2$ , H-24), 5.05 and 5.08 (2  $\times$  1H, 2 br s, H-26), 1.72 (3H, s, H-27), 0.79 (3H, s, H-28), 0.94 (3H, s, H-29), 0.87 (3H, s, H-30), 8.40 (1H, br s, OOH);  $^{13}\text{C}$ -NMR data, see Table 2; FABMS  $m/z$  481  $[\text{M} + \text{Li}]^+$ ; HRFABMS  $m/z$  481.3889 ( $\text{C}_{30}\text{H}_{50}\text{LiO}_4$ ,  $\Delta$  -2.0 mmu).

**Compound 11.** To a solution of **7** (8 mg) in  $\text{Et}_2\text{O}$  (2 mL) was added triphenylphosphine (15 mg). After being stirred for 2 h, the solution was evaporated to dryness and the residue chromatographed on Si gel (eluent, heptane–EtOAc 8:2) yielding **11** (3 mg). Amorphous powder:  $[\alpha]_{\text{D}} +51^\circ$  (*c* 0.2,  $\text{CHCl}_3$ );  $^1\text{H}$  NMR ( $\text{CDCl}_3$ )  $\delta$  3.19 (1H, m, H-3), 1.01 (3H, s, H-18), 0.15 (1H, d,  $J = 4$  Hz, H-19 $\alpha$ ), 0.34 (1H, d,  $J = 4$ , H-19 $\beta$ ), 0.89 (3H, d,  $J = 7$  Hz, H-21), 1.57 (1H, m, H-22a), 1.00 (1H, m, H-22b), 3.69 (1H, ddd,  $J = 6.5$ , 10.7, 1.7 Hz, H-23), 3.78 (1H, d,  $J = 6.5$ , H-24), 4.92 and 4.98 (2  $\times$  1H, 2 br s, H-26), 1.72 (3H, s, H-27), 0.96 (3H, s, H-28), 0.86 (3H, s, H-29); FABMS  $m/z$  451,  $[\text{M} + \text{Li}]^+$ ,  $\text{C}_{29}\text{H}_{48}\text{LiO}_3$ .

**Molecular Modeling Procedures.** Molecular modeling was carried out on a Silicon Graphics Indigo using BIOSYM software (BIOSYM/MSI). Initial models were generated using the builder module and refined *in vacuo* with a four-step procedure. The first stage consisted in relaxing the built models using steepest descent

followed by conjugate gradient minimizations. The second stage consisted in conformational space sampling using high-temperature (500 °K) dynamics simulation without experimental constraints. Structures were archived every 100 fs. The third stage was a quenching procedure including experimental constraints. Previous archived structures were cooled using two successive 200-fs dynamic simulations in a 0 °K coupled bath. The fourth stage consisted in lowering the potential energy of refined models using steepest descent and then conjugate gradient minimizations, with charges and experimental constraints.

**Experimentally Derived Constraints.** NOESY data (Table 1) were translated in three distance-restraint ranges according to their intensities: strong (2.0, 2.6 Å), medium (2.4, 3.4 Å), and weak (3.2, 5.0 Å). The use of pseudoatoms led to appropriate distance-restraint corrections.<sup>14</sup> Coupling constants (Table 1) were translated in dihedral angle-restraint ranges according to their intensities.<sup>15</sup>

## References and Notes

- (1) This work was performed in the framework of a collaborative program between the University of Malaya and CNRS.

- (2) Omobuwajo, O. R.; Martin, M.-T.; Perromat, G.; Sévenet, T.; Awang, K.; Pais, M. *Phytochemistry* **1996**, *41*, 1325–1328.
- (3) The previous name argenteanol<sup>2</sup> for compound **3** has been replaced by argenteanol A.
- (4) Isaev, M. I.; Gorovits, M. B.; Abubakirov, N. K. *Chem. Nat. Comp.* **1985**, *21*, 399–447.
- (5) H-17 and H-20 were superimposable in the spectrum measured in CDCl<sub>3</sub>. Conversely, H-16 and H-17 were superimposable in pyridine-*d*<sub>5</sub>. Thus, the NOESY correlation C-24/H-17 was deduced from experiments done in both solvents.
- (6) Ohmoto, T.; Ikeda, K.; Chiba, T. *Chem. Pharm. Bull.* **1982**, *30*, 2780–2786.
- (7) Khuong-Huu, F.; Sangare, M.; Chari, V. M.; Bekaert, A.; Devys, M.; Barbier, M.; Lukacs, G. *Tetrahedron Lett.* **1975**, *22*, 1787–1790.
- (8) Sheu, J. H.; Huang, S. Y.; Duh, C. Y. *J. Nat. Prod.* **1996**, *59*, 23–26.
- (9) For the *RS*, *SR*, and *SS* configurations, the number of violations per model greater than 0.1 Å of the NOE distance restraints was  $1.97 \pm 0.1$ ,  $1.92 \pm 0.24$ , and 3.0, respectively.
- (10) Yoshikawa, M.; Hatakeyama, S.; Tanaka, N.; Fukuda, Y.; Yamara, J.; Murakumi, N. *Chem. Pharm. Bull.* **1993**, *41*, 1948–1954.
- (11) Nakajima, Y.; Satoh, Y.; Katsumata, M.; Tsujiyama, K.; Ida Y.; Shohi, J. *Phytochemistry* **1996**, *41*, 1325–1330.
- (12) Cabrera, G. M.; Seldes, A. *J. Nat. Prod.* **1995**, *58*, 1920–1924.
- (13) Cabrera, G. M.; Seldes, A. *J. Nat. Prod.* **1996**, *59*, 343–347.
- (14) Wüthrich, K.; Billeter, M.; Braun, W. *J. Mol. Biol.* **1983**, *169*, 949–961.
- (15) Günther H., *NMR-Spektroskopie 3/E*, Georg Thieme Verlag: Stuttgart, 1992.

NP960594C